CONCRETE LIBRARY OF JSCE NO. 7, JULY 1986

Estimate of Strength and Deformation Characteristics of Reinforced Concrete Shell Elements Subjected to In-Plane Forces**

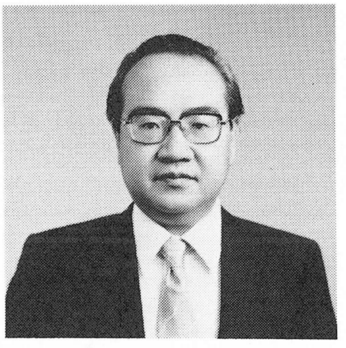

By Yukio AOYAGI*, Dr. of Eng.

SYNOPSIS

It is of importance to understand the stress-strain behavior of reinforcement and concrete and to consider it properly in the sectional design of reinforced concrete (RC) shell elements subjected to in-plane forces. Although some theoretical research has been conducted so far, little experimental data are available to substantiate the validity of proposed theories. With this in mind an experimental study was carried out, in which 24 models of orthogonally reinforced concrete shell plate elements were loaded by in-plane forces inclined to the directions of reinforcements, simulating the boundary conditions prevailing in the actual structures. Also, 7 hollow cylindrical models reinforced with orthogonal, three-way and four-way reinforcing systems were tested in torsion. Based on the experimental evidence that the direction of cracks and the average shear rigidity across cracks are dependent on ratios of orthogonal principal stresses and on crack widths, respectively, a simplified analytical procedure, by which the accuracy of the estimate could be improved, is presented.

** Reprint from the U.S-Japan Seminar on Finite Element Analysis of Reinforced Concrete Structures. May. 1985.

* Y. Aoyagi is a member of Japan Society of Civil Engineers, Japan Concrete Institute, ACI, etc. and is the head of material mechanics section at Civil Engineering Laboratory, Central Research Institute of Electric Power Industry, Chiba, Japan. He received his MS in 1964 and his Doctor of Engineering Degree in 1974 from the University of Tokyo, Japan. His research interests include design and construction of concrete containments for nuclear reactors, in-ground tanks for storage of LNG, prediction of cracking and deformational behaviors of reinforced concrete members under extremely low and elevated temperatures, creep, shrinkage and thermal effects on concrete structures, etc.

1. Introduction

Reinforced concrete (hereafter referred to as RC) shells have been applied to such structures as containments for nuclear power reactors, storage tanks for liquefied natural gas (LNG), water tanks, cooling towers, silos, etc. The field for application of RC shell structures is expected to increase also in the future. The design of RC shells has so far been based on sectional forces,which are induced by mechanical loadings such as internal pressure or earthquakes as well as restrained forces such as temperature effects. The internal forces are usually calculated by elastic analysis. The sectional forces are then utilized to determine the amount of reinforcement, taking into account the effect of cracking.

A typical critical stress condition occurs in an RC containment at the time of loss of coolant accident combined with an earthquake load. That is, the parts of the cylindrical wall parallel with the direction of earthquake force are likely to be subjected to combined stresses of N_x and N_y as well as N_{xy} (see Fig. -1).

This kind of problems was first studied in Germany in 1920s, and since the early part of 1970s it has become again one of the main themes of research interest not only in Germany but also in the USA, Japan, etc., because in connection with the construction of reinforced as well as prestressed concrete containments in high seismic regions, rationalization of design of an RC shell element against earthquake forces has become a problem requiring a solution. The present paper discusses the mechanical behavior of RC shell elements subjected to shearing stresses combined with in-plane membrane stresses, referring to the author's experimental results.

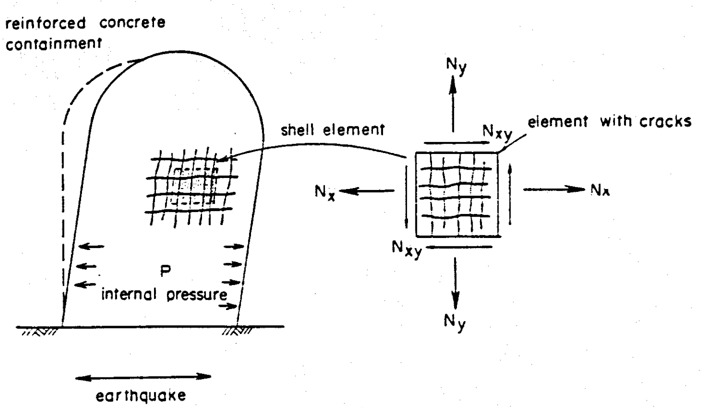

Fig.-1 Stress Conditions in Reinforced Concrete Containment Subjected to Earthquake with Presence of Internal Pressure

2. Specimens and Loading Method Employed by the Author

2.1 Test of Plate Specimens

Plate specimens with plan dimensions of test area 150 × 150 cm and a thickness of 10 cm (Fig. 2) were used for the test of orthogonally reinforced concrete shell elements. Around the periphery of specimen slitted thickened load introductory zones were attached to anchor the reinforcement and to facilitate uniform introduction of in-plane forces. The loads were applied by what is called a tournament scheme. 24 specimens were tested. Two percentages of steel were used and deviation angles of the principal forces with respect to the orthogonal reinforcement directions were varied from 0° to 45°. The disadvantages of this test method are the limited magnitude of shear forces applied to the specimens and the inability to introduce reversible shear stresses in the specimens. The main parameters of the specimens are listed in Table-1, together with the main test results.

2.2 Test of Cylindrical Models

To improve the controversial points of the above plate tests a reversal torsional loading test on RC hollow cylindrical models was conducted.

Configurations and dimensions of the test specimens are depicted in Fig.-3, together with loading scheme. Thickened stubs were monolithically connected to the cylindrical test area. Height, internal diameter and wall thickness were 200, 150 and 10 cm, respectively. Parameters varied in the specimens were the arrangements of the reinforcement as well as the ratio of reinforcement, and presence or absence of internal pressure. Main properties as well as concrete strengths of the models tested are listed in Table 2.

The inner face of the models, which were subjected to constant internal pressure, was lined with rubber sheet to keep the specimen watertight during the torsion test. After the internal pressure had attained the prescribed value, a torsion load was applied, sustaining the pressure up to failure by using a pressure, balancing nitrogen gas tank.

2:3 Materials used for Tests

The mix proportions of the concrete used for the experiment are shown in Table -3. Cylinder compressive strength of concrete at the time of test ranged from 200 to 280 kg/cm² for the cases of plate specimens. The yield point of the D-10 reinforcing bars used as the main reinforcing bars was 3780 kg/cm² and the tensile strength was 5510 kg/cm².

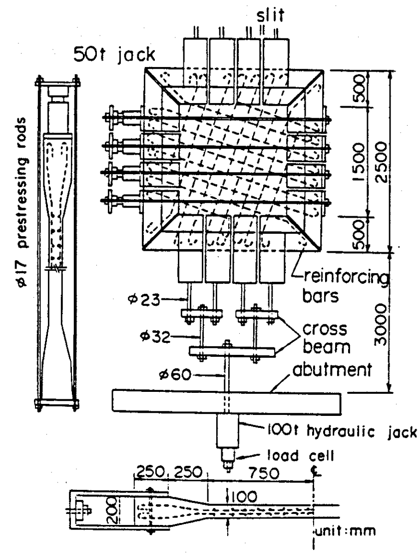

Fig.-2 Method of Applying In-plane Forces to Reinforced Concrete Plate Specimens Employed by the Author

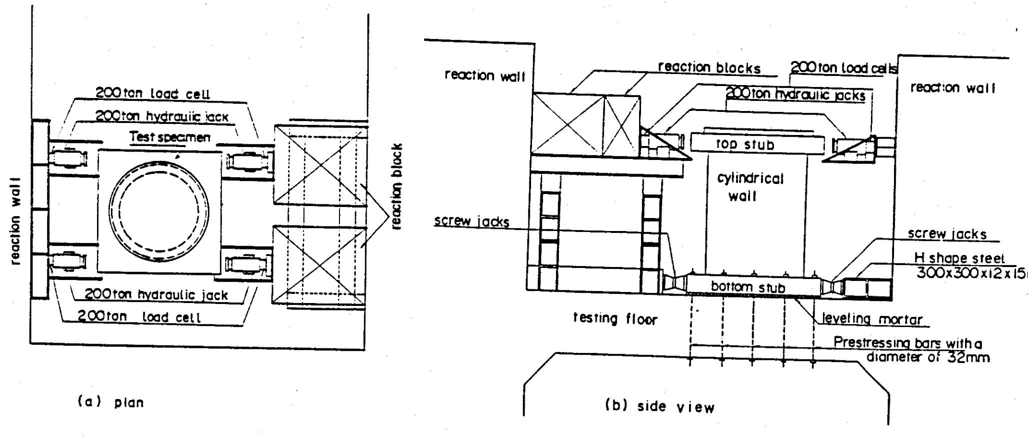

Fig.-3 Loading Scheme for RC Hollow Cylindrical Models

Table-1. Properties of Specimens and Comparisons of Calculated and Measured Yield Loads

No. of Specimens	Properties of specimen				N_1 Xyield	N_1 max	Leitz		Baumann		The Author				
	ρ (%)	α (°)	Presence of Crack	$k=\frac{N_2}{N_1}$			N_1 cal Xyield	Cal/ Mes.	N_1 cal Xyield	Cal/ Mes.	N_1 cal Xyield	Cal/ Mes.	N_1y, yield Cal	Mes	Cal/ Mes
20	0.761	0		0	44.0	63.5	43.2	1.02	43.2	1.02	43.2	1.02	-	-	-
6	0.761	0		0.5	40.0	64.0	43.2	0.93	43.2	0.93	43.2	0.93	-	-	-
11	0.713	12.5		0	44.0	56.0	35.7	1.23	37.2	1.18	38.6	1.14	56.0	40.5	1.38
12	0.713	12.5		1.0	38.0	46.0	40.5	0.94	40.5	0.94	40.5	0.94	42.0	40.5	1.03
7	0.713	22.5		0	36.0	50.0	33.5	1.07	36.1	1.00	35.6	1.01	44.0	40.5	1.09
8	0.713	22.5		0.5	36.0	48.0	36.7	0.98	37.4	0.96	35.0	1.03	41.0	41.3	1.00
9	0.713	22.5		1.0	36.0	44.0	40.5	0.89	40.5	0.89	40.5	0.89	44.0	40.5	1.09
13	0.713	22.5		-1.5	38.0	46.0	28.6	1.33	35.0	1.09	35.5	1.07	46.0	40.5	1.14
15	0.713	30		0.0	38.0	52.0	34.2	1.11	36.3	1.05	34.4	1.10	48.5	40.5	1.19
2	0.713	30		0	34.0	52.0	37.1	0.92	37.8	0.90	37.6	0.90	48.0	42.8	1.12
4	0.713	30		1.5	36.0	52.0	40.5	0.89	40.5	0.89	40.5	0.89	38.5	40.5	0.95
19	0.713	45		0.5	44.5	49.0	40.5	1.10	40.5	1.10	40.5	1.10	49.0	40.5	1.21
21	0.713	45		-1.0	42.0	51.5	40.5	1.04	40.5	1.04	40.5	1.04	51.5	40.5	1.27
3	0.713	30	ϕ=30	0.0	33.5	48.0	34.2	0.99	36.3	0.92	34.4	0.97	40.0	40.5	0.99
17	0.713	30	ϕ=57	0	47.5	56.0	37.1	1.28	37.8	1.26	37.6	1.26	47.0	42.8	1.10
10	0.713	22.5	ϕ=22.5	0	34.5	44.0	36.7	0.94	37.4	0.92	35.0	0.99	40.5	41.3	0.98
14	0.713	22.5	ϕ=22.5	-1.5	34.0	50.0	28.6	1.19	35.0	0.97	35.5	0.96	50.0	40.5	1.23
16	0.713	22.5	ϕ=49	-1	39.5	49.0	28.6	1.38	35.0	1.13	35.5	1.11	49.0	40.5	1.21
22	1.183	0		0	66.0	92.0	67.2	0.98	67.2	0.98	67.2	0.98	-	-	-
23	1.183	22.5		0	53.0	79.0	55.6	0.95	56.8	0.93	57.1	0.93	79.0	68.5	1.15
27	1.183	22.5		0	60.0	87.5	60.9	0.99	59.1	1.02	56.4	1.06	64.0	65.6	0.98
25	1.183	22.5	ϕ=22.5	0	51.0	82.5	55.6	0.92	56.8	0.90	57.1	0.89	82.5	68.5	1.20
26	1.183	45		0	61.5	82.0	67.2	0.92	67.2	0.92	67.2	0.92	69.0	67.2	1.03
24	x=1.183 y=0.592	22.5		0	51.0	65.0	55.6	0.92	52.5	0.97	54.2	0.94	58.5	57.0	1.03
	ϕ : Angle of the crack previously introduced (°)			average				1.04		1.00		1.00			1.11
				coefficient of variation				14.4%		9.6%		9.2%			10.1%

Table-2 Main Properties of the Cylindrical Specimens and Test Results

		Mark of Specimens	T-1.18 - 0.0	T-118A - 0.0	T-180 - 00	T-1.18T-0.0	T-1.80 - 35	T-1.18 - 3.0	T01.18T - 3.0
Reinforcing System		Arrangement of Deformed bars ϕ10 mm	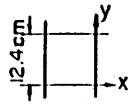 x.y : double	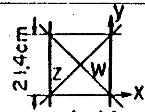 x.y : double w.z : single	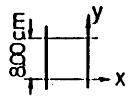 x.y : double	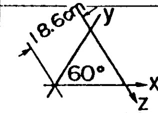 x.y.z : double	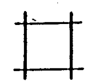 same as T-1.80-00	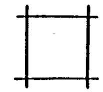 same as T.1.18-00	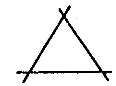 same as T.1.18T-00
	Ratio (%)	x bars	1.15	0.67	1.79	0.77	1.79	1.15	0.77
		y bars	1.15	0.67	1.79	0.77	1.79	1.15	0.77
		w,z bars	0	0.47	0	0.77	0	0	0.77
		Volumetric	2.30	2.28	3.58	2.31	3.58	2.30	2.31
Internal pressure (kg/cm^2)			0	0	0	0	3.5	3.0	3.0
Conc. streng		Comp(kg/cm^2)	297	352	367	287	336	290	2.67
		Tens(")	25.8	26.6	32.1	24.1	300	23.7	22.0
Tensile cracking stress due to internal pres.			-	-	-	-	24.5	19.3	19.3
Torsional Shear Stress at kg/cm^2		Cracking	19.2	20.2	21.1	18.1	7.4*	7.4*	5.7*
		Yielding in x	36.8	42.4	59.4	40.8	31.9	14.3	19.7
		in y	46.6	46.6	72.7	35.4	40.2	27.0	22.9
		in w or z	-	32.7	-	42.2	-	-	-
		Maximum τ_u	57.4	60.6	76.0	50.7	61.8	49.8	59.2
		$\tau_u/\sqrt{f'_c}$ **	3.32	3.22	3.96	2.99	3.37	2.92	3.62
Torsional deformation at τ_u (rad x 10^{-3})				23.7	83	20.8	2.38	37.6	48.8

* Shear stress at cracking due to torsion

** τ_u : Shear stress at ultimate (kg/cm^2) f'_c : concrete compressive strength (kg/cm^2)

3. Method of Analysis for RC Shell Element

3.1 Orthogonal Reinforcing System[12],[13],[14]

According to Baumann,[4] [5] stresses in the reinforcement as well as compressive forces in concrete struts can be estimated based on the equilibrium of forces acting on a preassumed crack surface. Because of the indeterminate nature of the equilibrium equations the angle of the crack with respect to y–reinforcement as well as shear forces occurring along the crack must be determined based either on the compatibility conditions for deformations or on experimentally obtained evidence. A statistical analysis of the crack angles ϕ (Fig.-6) up to yielding in x-reinforcement obtained through the tests of RC shell elements [15] showed that the main influencing factors on ϕ are the deviation angle of bars α (Fig.-6) and the value κ, defined as the ratio between the applied principal forces in both directions. That is, it was found to be practically justifiable to assume that in the domain of uniaxial tension to compression-tension ($\kappa \leq 0$), ϕ may be assumed equal to α, while at the point of equal biaxial tension ($\kappa = 1$), ϕ may be fixed at an angle of 45° regardless of the values of α. In the intermediate region ($0 < \kappa < 1$) ϕ can be linearly interpolated in terms of κ as illustrated in Fig.-4.

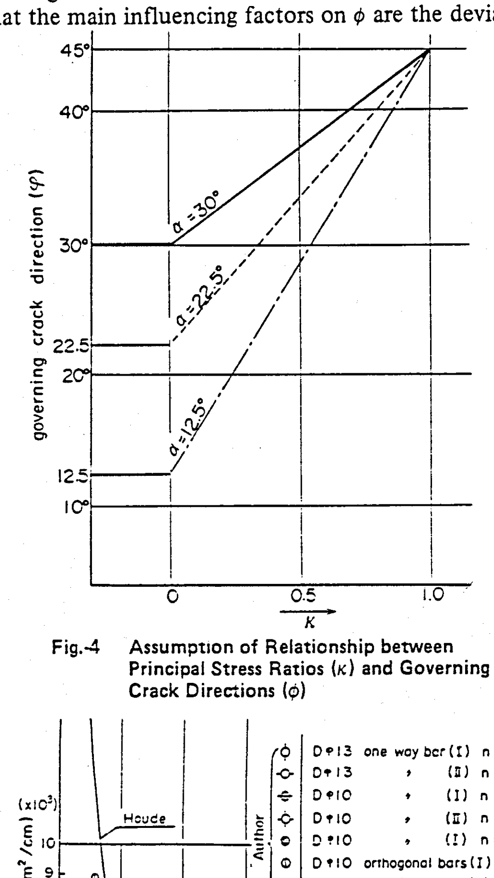

Fig.-4 Assumption of Relationship between Principal Stress Ratios (κ) and Governing Crack Directions (ϕ)

Unknown shear force transferred across the crack, S, is calculated in the same way as was proposed by Baumann.[4],[5] However, G_{cr}, which is defined as average shear rigidity across cracks, is experimentally determined. Referring to the results of the push-off tests obtained by the author et al. (see Fig.-5)[15] on precracked reinforced concrete blocks, G_{cr} could be approximated as a function of crack widths as follows:

$$G_{cr} = \frac{36}{w_m} \ell_m = \frac{36}{\epsilon_{\phi m}} \text{ (kg/cm}^2\text{)} \quad (1)$$

where, w_m : average crack width in cm. ℓ_m : average crack spacing $\epsilon_{\phi m}$: average strain perpendicular to the direction of crack.

w_m is, on the other hand, a function of the average strains of shell element perpendicular to the direction of cracks. w_m is calculated by multiplying the average strain $\epsilon_{\phi m}$ by the average

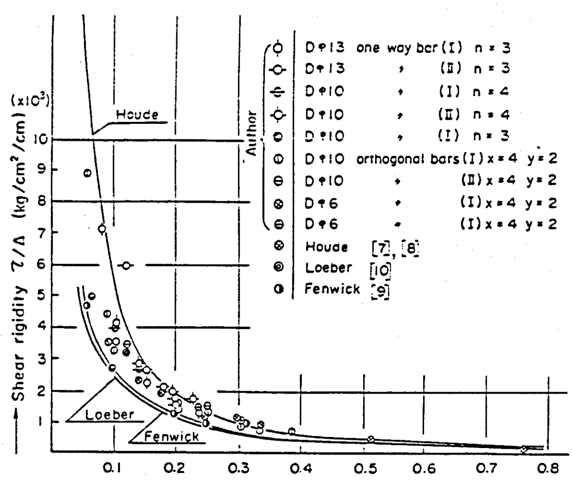

Fig.-5 Experimental Relationship between Widths of Cracks and Shear Rigidities

Table-3. Mix. Proportion of Concrete used for Experiment

Mix Proportion

Water cement ratio (%)	Ratio of fine aggregate (%)	Slump (cm)	Air content (%)	Unit content (kg/m^3)					
				Water	Cement	Fine aggregate	Coarse aggregate 10 - 20 mm	Coarse aggregate 5 - 10 mm	Pczzolith No. 51
77	52	10±1	3±1	179	332	966	626	313	0.580

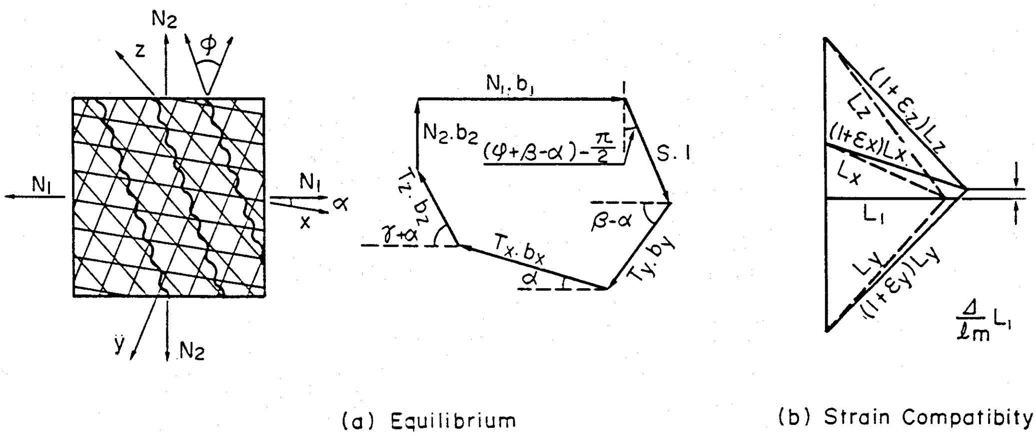

Fig.-6 Equilibrium of Forces and Strain Compatibility in Three Way RC Shell Element

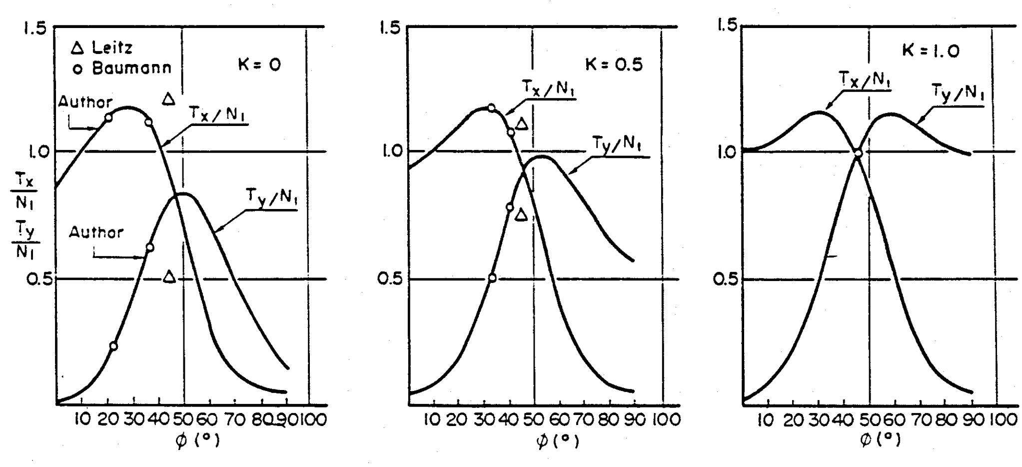

Fig.-7 Relationships between ϕ and T_x/N_1 as well as T_y/N_1 Obtained by Leitz, Baumann and the Author (α=22.5°, ρ_x=0.713%, N_1=30tons)

strain $\epsilon_{\phi m}$ by the average crack spacing ℓm. $\epsilon_{\phi m}$ can be predicted using the following equations (2), also developed by Baumann.[4],[5]

$$\epsilon_\phi = \frac{\epsilon_x}{\cos^2\phi} + \frac{\Delta}{\ell_m}\tan\phi = \frac{\epsilon_y}{\sin^2\phi} - \frac{\Delta}{\ell_m}\cot\phi$$

$$\epsilon_\phi = \epsilon_x + \epsilon_y$$

$$\Delta/\ell_m = \epsilon_y\cot\phi - \epsilon_x\tan\phi$$

$$\epsilon_1 = \epsilon_\phi\cos^2(\phi-\alpha) - \sin(\phi-\alpha)\cdot\cos(\phi-\alpha)\Delta/\ell m$$

$$\epsilon_2 = \epsilon_\phi\sin^2(\phi-\alpha) + \sin(\phi-\alpha)\cdot\cos(\phi-\alpha)\Delta/\ell m \qquad (2)$$

In the formula to relate the average strains in the reinforcement to those at a cracked section, trial fitting of the experimental data to the estimated[15] led to a modification of the original CEB formula. That is, in the modified equation the exponent of the second term of CEB formula was changed to 3 in lieu of the original 2. This may explain the fact that in a shell element, subject to membrane forces, degradation of bond between concrete and steel proceeds more rapidly than in ordinary RC beams or slabs, subject to flexural moment. The resulting equations adopted are as follows; [15]

$$\epsilon_{xm} = \epsilon_x\left[1 - \left(\frac{\sigma_{x,cr}}{\sigma_x}\right)^3\right]$$

$$\epsilon_{ym} = \epsilon_y\left[1 - \left(\frac{\sigma_{y,cr}}{\sigma_y}\right)^3\right] \qquad (3)$$

The crack spacing can be obtained by applying formulas such as provided in CEB Code. From the equilibrium of forces, the following equation is derived, which relates the sum of the forces in reinforcement in both directions to shear forces along the crack S.

$$T_x + T_y = (N_1+N_2) + (N_1-N_2)\sin\alpha\cdot\cos\alpha(\tan\phi) + S(\tan\phi-\cot\phi) \qquad (4)$$

As the crack angle ϕ is automatically given by the deviation angle α and external stress ratio κ, the problem is reduced to the determination of only S. The computation can be conducted by an iterative process.

3.2 Three Way Reinforcing System

Suppose a triangularly reinforced concrete shell element (Fig.-6) is loaded by biaxial principal membrane forces N_1 and N_2, the equilibrium of forces acting on the crack plane and the corresponding polygon of forces can be depicted as in Fig.-6(a). Also, the conditions of strain compatibility in x, y and z reinforcements at the cracked section can be drawn as in Fig.-6(b), neglecting the compressive strain in the concrete strut.

Referring to Fig.-6(b), the strain in z-reinforcement is expressed by the following equation.

$$\epsilon_z = [\epsilon_x\sin(\beta+\gamma)/\sin(\phi+\beta) - \epsilon_y\sin\gamma/\sin\phi] \times \sin(\phi+\beta+\gamma)/\sin\beta \qquad (5)$$

Based on the force equilibrium shown in Fig.-6(a), T_x, T_y and T_z, which denote the tensile forces in x, y and z reinforcements per unit width of shell element, respectively, can be expressed as follows:

$$
\begin{aligned}
T_z &= [\lambda_x T_x \sin(\beta+\gamma)/\sin(\phi+\beta) - \lambda y T_y \sin\gamma/\sin\phi] \cdot \sin(\phi+\beta+\gamma)/\sin\gamma \\
T_x &= (bN_1 + cN_2 + dS)/a \\
T_y &= (fN_1 + gN_2 + hS)/e
\end{aligned} \qquad (6)
$$

where $\lambda_x = \rho_z/\rho_x$, $\lambda_y = \rho_z/\rho_y$, ρ_x, ρ_y, ρ_z : reinforcement ratios in x, y and z directions respectively, α, β, γ : angle of the x, y and z reinforcements with respect to the principal force N_1, ϕ : angle between the directions of y–reinforcement and crack.

The coefficients appearing in the equation (6) are as follows:

$$
\begin{aligned}
a &= \sin(\phi+\beta) \cdot \sin^2\beta \cdot \sin\phi + \lambda_x \sin^2(\phi+\beta+\gamma) \cdot \sin^2(\beta+\gamma)\sin\phi / \\
&\quad \sin(\phi+\beta) + \lambda_y \sin^2(\phi+\beta+\gamma) \cdot \sin^2\gamma \cdot \sin(\phi+\beta)/\sin\phi \\
b &= \sin(\phi+\beta-\alpha) \cdot \sin(\beta-\alpha) \cdot \sin\beta \cdot \sin\phi + \lambda_y \sin^2(\phi+\beta+\gamma) \times \\
&\quad \sin(\phi+\beta-\alpha) \cdot \sin\gamma \cdot \sin(\alpha+\gamma)/\sin\phi \\
c &= \cos(\phi+\beta-\alpha) \cdot \cos(\beta-\alpha) \cdot \sin\phi \cdot \sin\beta - \lambda_y \cos(\phi+\beta-\alpha) \times \\
&\quad \sin^2(\phi+\beta+\gamma) \cdot \sin\gamma \cdot \cos(\alpha+\gamma)/\sin\phi \\
d &= \sin^2\phi \cdot \sin\beta + \lambda_y \sin^2(\phi+\beta+\gamma) \cdot \sin\gamma \cdot [\sin\phi \cdot \sin\gamma - \sin(\phi+\beta) \times \\
&\quad \sin(\beta+\gamma)]/\sin\phi \cdot \sin\beta \\
e &= \sin\phi \cdot \sin(\phi+\beta) \cdot \sin^2\beta + \lambda_x \sin^2(\phi+\beta+\gamma) \cdot \sin^2(\beta+\gamma) \cdot \sin\phi / \\
&\quad \sin(\phi+\beta) + \lambda_y \sin^2(\phi+\beta+\gamma) \cdot \sin_2\gamma \cdot \sin(\phi+\beta)/\sin\phi \\
f &= \lambda_x \sin^2(\phi+\beta+\gamma) \cdot \sin(\phi+\beta-\alpha) \cdot \sin(\beta+\gamma) \cdot \sin(\alpha+\gamma) / \\
&\quad \sin(\phi+\beta) + \sin(\phi+\beta-\alpha) \cdot \sin\alpha \cdot \sin(\phi+\beta) \cdot \sin\beta \\
g &= -\lambda_x \sin^2(\phi+\beta+\gamma) \cdot \cos(\phi+\beta-\alpha) \cdot \sin(\beta+\gamma) \cdot \cos(\alpha+\gamma) / \\
&\quad \sin(\phi+\beta) - \cos(\phi+\beta-\alpha) \cdot \cos\alpha \cdot \sin(\phi+\beta) \cdot \sin\beta \\
h &= \lambda_x \sin^2(\phi+\beta+\gamma) \cdot \sin(\beta+\gamma) \cdot [\sin\phi \cdot \sin\gamma - \sin(\phi+\beta) \cdot \sin(\beta+\gamma)] / \\
&\quad \sin(\phi+\beta) \cdot \sin\beta - \sin^2(\phi+\beta) \cdot \sin\beta
\end{aligned}
$$

The shear stress transferred across crack ,τ, , the shear force per unit width of shell element ,S, and the average shear rigidity of the shell element, G_{cr}, may be expressed as follows:

$$
\begin{aligned}
\tau &= G_{cr} \cdot \Delta/\ell_m \\
S &= \tau \cdot d \\
G_{cr} &= 36/\epsilon_{\phi m} \ (\mathrm{kg/cm^2})
\end{aligned} \qquad (7)
$$

where Δ: relative shear slip between edges of a crack, ℓ_m : average crack spacing, d: thickness of shell element.

Averaged normal strain in the direction perpendicular to cracks ($\epsilon_{\phi m}$) and relative shear slip divided by crack spacing (Δ/ℓ_m) are given as functions of ϵ_{xm} and ϵ_{ym}, which are average strains in x and y reinforcements, respectively.

$$\begin{aligned} \epsilon_{\phi m} &= \epsilon_{xm} \cos\phi/\sin(\phi+\beta) \cdot \sin\beta - \epsilon_{ym} \cos(\phi+\beta)/\sin\phi \cdot \sin\beta \\ \Delta/\ell_m &= -\epsilon_{xm} \sin\phi/\sin\beta \cdot \sin(\phi+\beta) + \epsilon_{ym} \sin(\phi+\beta)/\sin\phi \cdot \sin\beta \end{aligned} \tag{8}$$

are defined independently as a function of principal stress ratio $\kappa = N_2/N_1$, as is described in the Section 3.1. Substituting the value of ϕ in the above equations, T_x, T_y, T_z and S are computed by solving interatively the simultaneous equations of (6) and (7).

The analytical procedure is also applicable to four way reinforcing system, when the reinforcement in one of the four directions is stressed in compression.

4. Verification of Analytical Method

4.1 An Example of Comparisons of Analytical Results Obtained by Various Authors

According to Flügge's formula,[2] if an RC shell element with a ratio of the reinforcements in the two directions $\lambda = \rho_x/\rho_y = 3$ is subjected to uniaxial tension with an angle of deviation $\alpha = 30°$, then the stresses in both reinforcements become identical, which also correspond to the minimum volume of reinforcements under the given loading conditions. To compare the analytical results among various proposed methods, T_x, T_y, R and S were calculated and are summarized in Table-4. In the table N_I is the value of principal stress in concrete occurring between the two adjacent cracks. R is the stress in the compressive strut.

Since in the author's as well as Tsubaki's formulas[6] absolute values of reinforcement ratios in both directions are required, ρ_x and ρ_y are assumed to be 1.18%, and 0.39%, respectively. The dimensions of the shell element was assumed to be the same as that of author's plate specimens, and the load considered for calculation was fixed as N_1 = 30 tons. The coefficients used in Tsubaki's formula are assumed as $\mu = 1.7$ and $\alpha_d = 1.0$.

Referring to the dimensionless values of forces in the x-reinforcement expressed by T_x/N_1, some differences can be recognized among the methods compared, the values being scattered in the range from the minimum of Flügge's 0.75 to the maximum of Baumann's 1.29. To the contrary, the values related to the y-reinforcement T_y/N_1 show an extremely wide difference such as that between Peter's[3] 0.15 and Tsubaki's 15.10. This is because Tsubaki assumes the cracks being nearly parallel to the y-reinforcement, increasing the steel stress extraordinarily due to friction, which, however, is inconceivable in practical situations. Even if disregarding Tsubaki's theory, considerable differences are observed in the stresses of the y-reinforcement among the researchers, ranging from Peter's 0.15 to Leitz's 0.68.

Looking at the stress in concrete strut R/N_1, somewhat higher values are obtained from Baumann and Leitz[1] than from Peter and the author. This implies that the direction of the assumed cracks plays an important role for the stress of concrete strut. As for shear force transferred along the cracked plane, Flügge, Peter and the author give approximately the same results. The fact that Flügge's value for N_I/N_1 is the largest one reflects his basic preposition that all the shear stresses are transmitted through aggregate interlock. Similar values are obtained by Peter and the author for all of the above parameters.

The above comparison led to the conclusion that although there are no significant differences among the methods hitherto proposed for the stresses in the x-reinforcement which has a smaller angle with the larger external principal tensile force, discrepancies are noted for the y-reinforcement.

Therefore, the author investigated the dependence of stresses in reinforcement on the crack inclinations. The calculations were conducted by the author's method for the

Table-4. Comparisons of Calculated Results from Various Analytical Methods **(α=30°, $\kappa=N_2/N_1$=0, $\lambda=\rho_x/\rho_y$=3)**

Analytical Methods	Assumption of Crack Formation	$\frac{T_x}{N_1}$	$\frac{T_y}{N_1}$	$\frac{R}{N_1}$	$\frac{S}{N_1}$	$\frac{N_I}{N_1}$
Flügge ; Orthogonal two-way cracking ϕ= 0 and ϕ= 90°	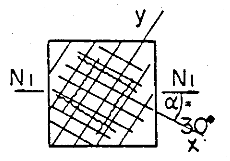	0.75	0.75	0.00	0.43	0.43
Leitz ; ϕ = 45° χ = ∞	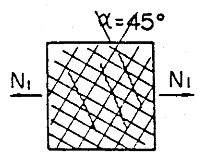	1.18	0.68	0.87	0	0
Peter ; Cracks perpendicular to principal force N_1 $\phi=\alpha$=30° χ=0	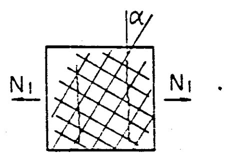	1.28	0.15	0.43	0.49	0.32
Baumann ; Principle of least deformation energy $\phi=\phi_1$ χ: variable	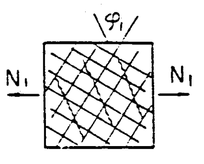	1.29	0.61	0.90	0	0
Tsubaki ; Shear friction theory ϕ=1° χ: variable	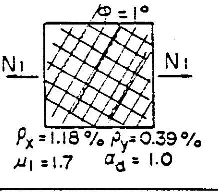	0.89	15.10	14.8	0.23	0
The author ; $\phi=\alpha$=30° χ: variable	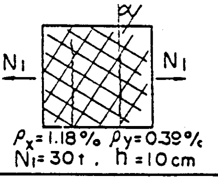	1.26	0.22	0.50	0.44	0.26

particular parameters of RC shell elements, that is, $\rho_x=\rho_y=0.713\%$, $\alpha=22.5°$ and $\kappa=0$, 0.5 and 1.0. The results are expressed in Fig. 7 as the relationship between ϕ and the dimensionless parameters T_x/N_1 and T_y/N_1, together with Baumann's and Leitz's estimations.

As can be seen from the figure, in the domain of angle ϕ from 20°~45°, for which practical designs are generally made, the inclinations of the curves for T_y/N_1 are so steep that the stresses in the y-reinforcement are far more sensitive to the direction of cracks assumed than those in the x-reinforcement. Coincidence of the calculated results by the three methods is only attained for the case of equal biaxial tension ($\kappa=1$). This again shows the importance of assigning the crack angles as true as possible to the actual conditions in the estimation of stresses in the y-reinforcement.

4.2 Comparisons of Plate Specimens

4.2.1 Average strains in reinforcements

In Fig.-8 the steel strain variation of the No.23 specimen averaged over a length spanning several cracks, versus the load is compared with those calculated by the methods proposed by Leitz, Baumann and the author. While the calculated strains in the x direction are practically identical among the three methods and provide a good fit to the measured, in the y direction the agreement seems distinctively better for the author's than the other two methods. Substantially the same results of comparisons were obtained for the cases of the unbalanced reinforced specimen (No. 24) subjected to uniaxial tension as well as the equally reinforced specimen (No. 27) subjected to biaxial tension.

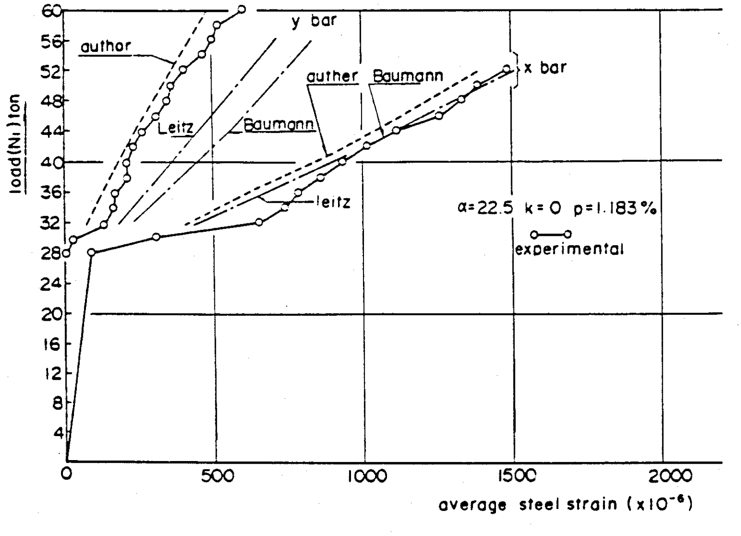

Fig.-8 **Comparison of Measured Average Strains in Steels with Calculated**

4.2.2 Yielding load in the x (weaker) direction.

The ratios of calculated and measured loads causing yielding in the x-bars are shown in Table-1 as well as in Fig.-9 in terms of principal stress ratios of κ. It can be seen that although there are no distinct differences between the accuracies of prediction obtained by Baumann and the author over the range of κ investigated, Leitz's theory has a tendency to underestimate the test results in the compression-tension region, especially at the value of κ equal to -1, that is, pure shear.

4.2.3 Deformations in the N_1 direction and shear slip

Fig.-10 shows comparisons of measured average post-cracked deformations in the direction of the principal tensile force N_1 with the results computed by the author for the cases of α=0°, 22.5° and 45°. The deformations, which become remarkably larger with increase in deviation angle ϕ, can also be predicted fairly well by the analytical procedure proposed by the author.

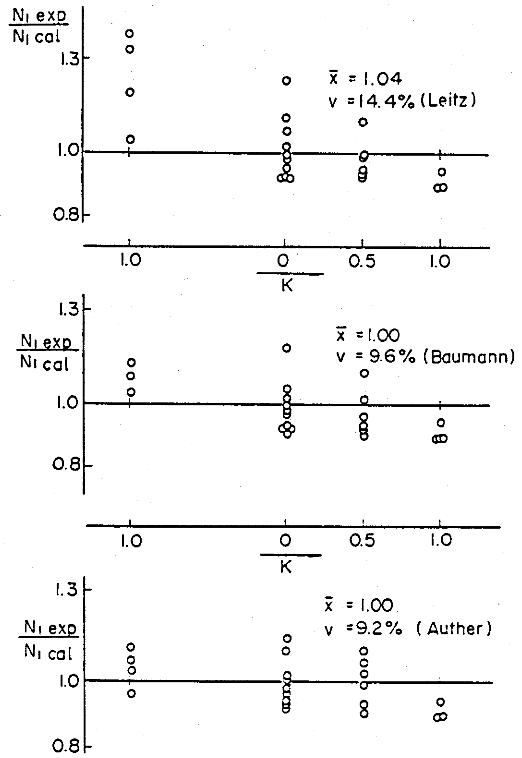

Fig.-9 Ratios of Calculated and Measured Loads Causing Yield in x Bars

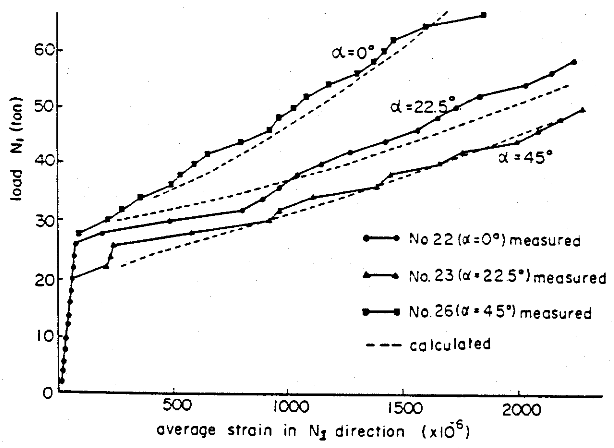

Fig.-10 Comparison of Measured Deformations in N_1 Direction with Calculated Deformations.

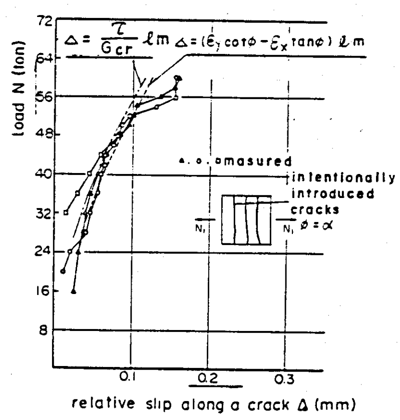

Fig.-11 Comparison of Measured Relative Slips along a Crack with Calculated No.25

In Fig.-11 relative shear slips along a crack are plotted against the applied principal force N_1, together with the calculated values based on the data of push-off tests as well as derived by the theoretically obtained strains in the reinforcement. It seems that the two estimates give similar results with a good fit of the experimental values. This seems to support the validity of the assumption adopted for the evaluation of the shear rigidities.

4.2.4 The load causing yielding in the y (stronger) reinforcement

The author derived a formula to predict the load causing yielding in the y reinforcement based on the theory mentioned before. In this analysis an assumption was made that after the x-reinforcement has yielded the load increment is to be resisted only by the stress increase in the y-reinforcement and the shear to be transferred across the crack S. The crack angle ϕ was assumed to retain its original value in the pre-yielding stage. The resulting formula to calculate the load increment required to cause yielding in the y reinforcement is obtained as follows:[15]

$$\Delta N_1 = \Delta T_y \tan^2\phi / [\cos^2\alpha \cdot (1 + \tan\alpha\tan\phi)^2 + \kappa \sin^2\alpha \cdot (1 - \cot\alpha\tan\phi)^2] \qquad (9)$$

where ΔN_1 : increase of the principal force N_1 per unit width of the plate element after yielding in the x-reinforcement.

$\Delta T_y = T_y^{yield,y} - T_y^{yield,x}$

$T_y^{yield,y}$: yield capacity per unit width in the y direction

$T_y^{yield,x}$: the y directional force per unit width when the x-reinforcement ment just yielded

The ratios between measured and calculated values of loads causing yielding in the y direction are listed in Table-1. An average ratio between experimental and calculated of 1.11 and a coefficient of variation of 10.1% suggest applicability of the proposed procedure.

4.3 Comparisons of Cylindrical Models

Effects of the reinforcing systems, reinforcement ratios and presence of internal pressure on the experimental torsional deformation behaviors can be seen on the skeleton curves for all the cylindrical models tested. (see Fig. 12)

In Figs-13 to 15 measured and calculated results for torsional deformations are shown for all of the tested specimens. Calculated torsional shear stresses at which first yielding of the steel occurs are listed in Table-2 together with the experimental results.

Fairly good agreements of the author's computed results with experimental results warrant the validity of the analytical method for the practical design purposes of RC shell elements subjected to in-plane shear combined with membrane tension. The range of applicability of the method should, however, be restricted up to the loading level, at which any of the reinforcements in the shell element starts to yield. Also, the preceding membrane cracks caused by internal pressure were found to affect markedly the deformational behaviours of shell elements, pointing out the necessity of further study directed to the behaviours of a shell element with pre-existing multi-directional cracks.

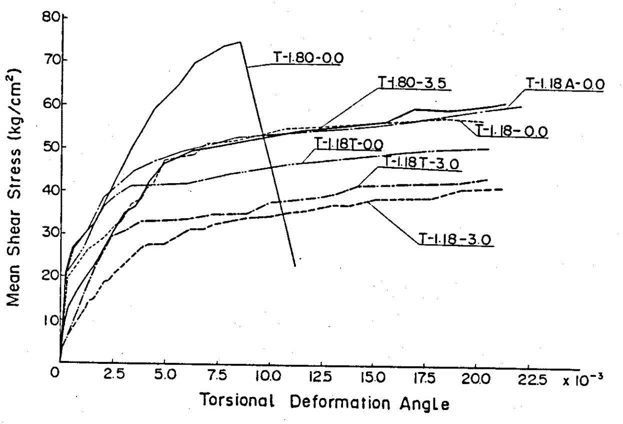

Fig.-12 Skeleton Curves of Torsional Deformations for all the Cylindrical Models Tested

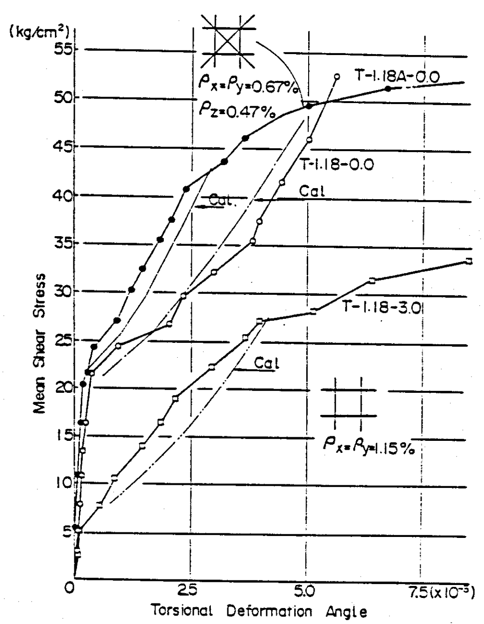

Fig.-13 Comparison of Torsional Deformation Angle as Measured and Calculated by the Author (Orthogonal and four way ρ_V. 2.3%) (ρ_V: volumetric percentage of steel)

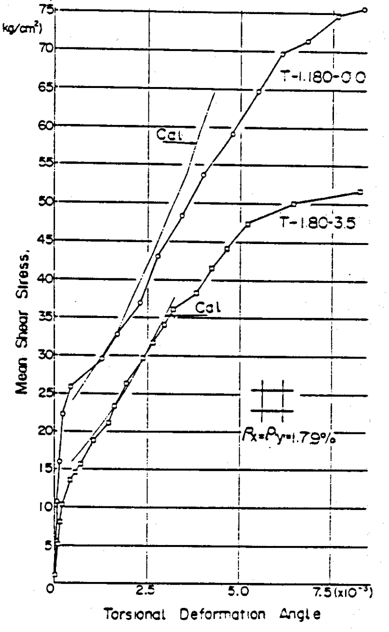

Fig.-14 Comparison of Torsional Deformation Angle between Measured and Calculated by the Author (Triangular ρ_V=2.31%)

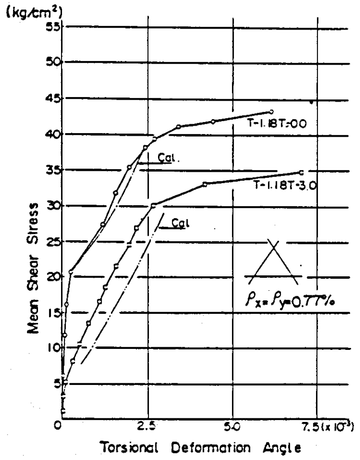

Fig.-15 Comparison of Torsional Deformation Angle as Measured and Calculated by the Author (Triangular ρ_v=2.31%)

5. Application of Finite Element Method

5.1 Outline of FEM Analysis

In the previous section the applicability of the author's practical method of analysis to the three as well as four way reinforcing systems was confirmed. In this section, mention of a trial use of a finite element plane stress crack analysis for estimating the mechanical behavior of the tested models is given.

Finite meshes of shell elements were selected so that the reinforcing bars are positioned just at the boundaries of adjacent elements. Concrete and reinforcing bars were modeled using 8 node isoparametric plane elements and 3 node isoparametric truss elements, respectively. Young's modulus, Poisson's ratio, yielding point and post yielding strain hardening rate were assumed as $E_s=1.98\times10^6$ kg/cm², $\nu=0.3$, $\sigma_{sy}=3900$kg/cm² and $H'=E_s/100$, respectively. Kupfer's[11] constitutive equation for plane stress, which was modified by the author's test results, was utilized.

The basic assumptions concerning the effects of cracks are as follows;

(1) After the formation of the cracks the stress drops to zero, and tensile axial rigidities in the direction perpendicular to the crack also becomes zero.

(2) Cracks do not change the material properties determining the axial rigidities in the direction parallel to the crack.

(3) Average shear rigidities across cracks are dependent on the crack widths in the same manner as described in section 3.1, that is, $G_{cr}=36/\epsilon_{\phi m}$ (kg/cm²).

In the process of computation torsional loads were applied monotonically in steps with an increment of 10 tons, except for the loading stage immediately after cracking, when a negligibly small increment was added.

5.2 Comparisons of Test Results with the Computed Results.

Experimental hysteretic curves for torsional deformations and corresponding calculated skeleton curves are shown in Fig.-16 to 18, for the three specimens subjected to pure torsion without internal pressure. It may be seen that the analytical curves follow fairly well the experimental tendencies up to a larger torsional angle of nearly 10×10^{-3} rad, that is 2 to 3 times as large as that at the first yielding of the steel, indicating the applicability of the FEM even in the post-yielding range of shear deformations.

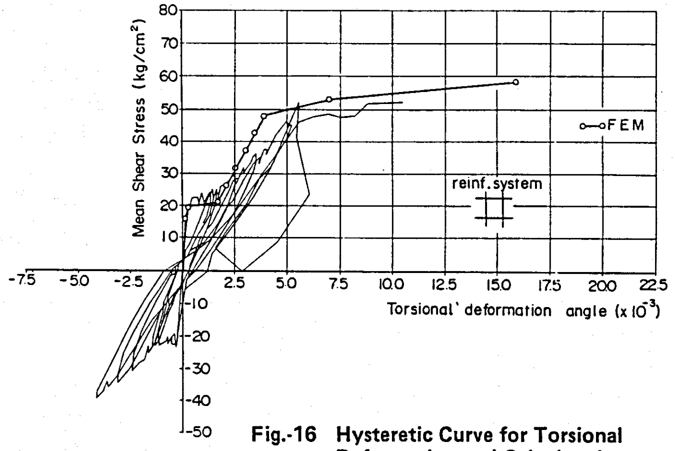

Fig.-16 Hysteretic Curve for Torsional Deformation and Calculated Skeleton Curve (T-1.18-0.0)

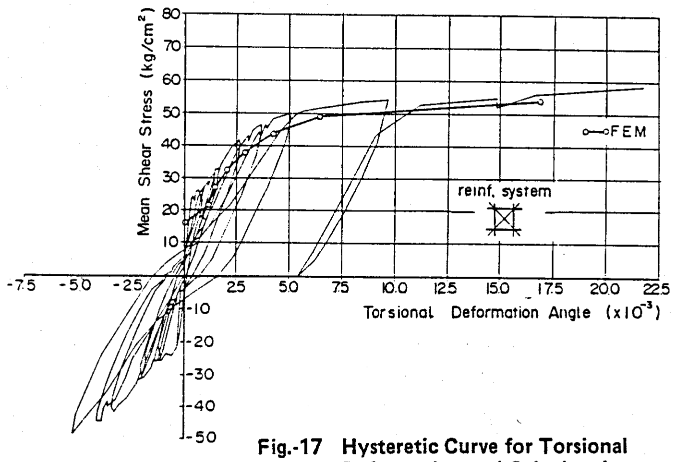

Fig.-17 Hysteretic Curve for Torsional Deformation and Calculated Skeleton Curve (T-1.18A-0.0)

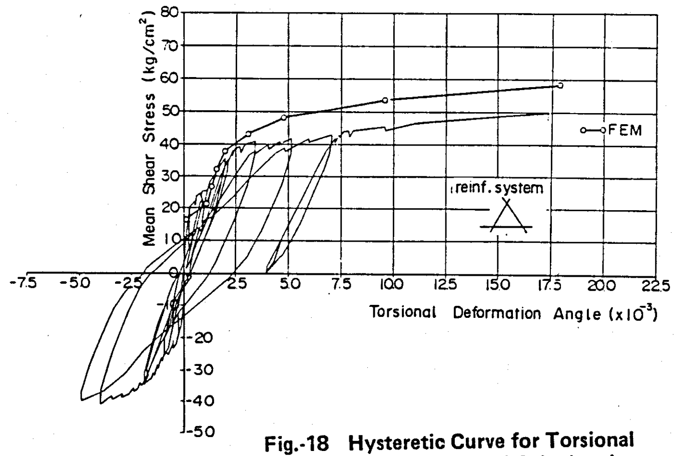

Fig.-18 Hysteretic Curve for Torsional Deformation and Calculated Skeleton Curve (T-1.18T-0.0)

6 Conclusions

Experimental results for the reinforced concrete plate specimens tested under in-plane force and hollow cylindrical models subjected to torsion were reviewed with particular reference to clarification of mechanical behavior as well as rationalization of the design method for RC shell elements.

The main conclusions obtained within the limitations of this study are:

(1) As a method for calculating the stress and deformation of RC shell elements, using the method of Baumann as the basis, an analysis procedure was proposed in which the stress dependence of cracking direction described previously, the crack width dependence of the shearing rigidity transfered through crack edges, and the contribution of the concrete portion between cracks to the tensile rigidity were taken into consideration. It was confirmed that the results of analysis by this procedure showed better agreement with the measured values than the calculated values of the stress, deformation and crack width by the procedures proposed by other authors. In particular, for the calculation in the stress of reinforcing bars which make a larger angle with the larger principal tensile stress (y-reinforcing bars), it was shown that the applicability of the equations proposed by the author was especially good.

(2) Experimental evidence showed that for the case of a constant volumetric reinforcement ratio, an orthogonal reinforcing system combined with diagonal bars and a triangular reinforcing system are advantageous for the loading conditions of pure shear and of shear plus membrane tension, respectively, from the view point of strength as well as deformational characteristics.

It was confirmed that the author's analytical method originally proposed for orthogonal bar networks is applicable to three as well as four way reinforcing arrangements with the limitation that the loading level considered should be lower than that causing yielding in the steel.

(3) A finite element analysis considering the effect of cracks was found to be effective to estimate the mechanical behavior of RC shell elements subjected to pure shear up to a state of shear deformation far beyond the yielding.

References

[1] Leitz, H. : "Eisenbewehrte Platten bei allgemeinen Biegungszustanden", Bautechnik, Heft 32, 1923.

[2] Flügge, W.: "Statik und Dynamik der Schalen", 3rd ed., Berlin, Springer-Verlag, 1962.

[3] Peter, J. : "Zur Bewehrung von Scheiben und Schalen für Hauptspannungen Schiefwinklig zur Bewehrungsrichtung", Die Bautechnik, Vol. 43, No. 5, pp. 149–154, 1966, and Vol. 43, No. 7, pp. 240–248, 1966.

[4] Baumann, T. : "Zur Frage der Netzbewehrung von Flachentragwerken", Der Bauingenieur, Vol. 47, Heft 10, pp. 367–372, 1972.

[5] Baumann, T. : "Tragwirkung Orthogonaler Bewehrungsnetze beliebiger Richtung in Flachentragwerken aus Stahlbeton", Deutcher Ausschuss für Stahlbeton, Heft 217, Berlin, 1972.

[6] Bazant, Z.P. and T. Tsubaki : "Concrete Reinforcing Net: Optimum Slip-Free Limit Design, Proc. of ASCE, Vol. 105, No. ST2, pp. 327–346, February 1979.

[7] Houde, J. : "Study of Force-Displacement Relationship for the Finite Element Analysis of Reinforced Concrete", Structural Concrete Series, No. 73-2, McGill University, Montreal, December 1973.

[8] Mirza, M.S. and J. Houde : "A Finite Element Analysis of Shear Strength of Reinforced Concrete Beams", ACI Special Publication SP 42-5, Vol. 1, "Shear in Reinforced Concrete", Detroit, Michigan, pp. 103–128, 1974.

[9] Fenwick, R.C. and T. Paulay : "Mechanisms of Shear Resistance of Concrete Beams", Journal of Structural Division, ASCE, Vol. 94, No. ST10, Proc. Paper 2325, pp. 2325–2350, October 1968.

[10] Loeber, P.J. : "Shear Transfer by Aggregate Interlock", M.E. Thesis, University of Canterbury, Christchurch, New Zealand, 1970.

[11] Kupfer, H. : "Das nicht lineare Verhalten des Betons bei zweiachsiger Beanspruchung", Beton und Stahlbetonbau, Heft 11, 1973.

[12] Aoyagi, Y. and K. Yamada : "An Experimental Approach to the Design of Network Reinforcement against In-plane Shear in Reinforced Concrete Containments", 5th SMIRT Conference, J4/7, Berlin, Germany, 1979.

[13] Aoyagi, Y., S. Ohmori and K. Yamada : "Strength and Deformational Characteristics of Orthogonally Reinforced Concrete Containment Models Subjected to Lateral Forces", 6th SMIRT Conference, J4/5, Paris, France, 1981.

[14] Aoyagi, Y. : "Analytical Approach to the Design of Orthogonally Reinforced Concrete Shell Elements Subjected to In-plane Shear", Proc. of JCI Colloquium on Shear Analysis of RC Structures, June 1982.

[15] Aoyagi, Y. and K. Yamada : "Strength and Deformational Characteristics of Reinforced Concrete Shell Elements Subjected to In-plane Forces", Concrete Library of JSCE, No. 4, Dec. 1984.

Aknowledgement

The author expresses his deepest appreciation to Dr. H. Okamura, Professor of University of Tokyo, and to Dr. K. Yamada, Chief Research Engineer, Maeda Construction Company, for their helpful suggestions and kind cooperation.